Sensors and Materials, Vol. 37, No. 12 (2025) 5411–5424
MYU Tokyo

S & M 4253

Eye–hand Coordination Simulator of Robot Arms for Science, Technology, Engineering, and Mathematics Education

Pimpran Preedanont and Pitikhate Sooraksa*

Department of Robotics and AI, School of Engineering, King Mongkut's Institute of Technology Ladkrabang,
1 Soi Chalongkrung 1, Ladkrabang, Bangkok 10520, Thailand

(Received September 30, 2025; accepted October 14, 2025)

Keywords: STEM education, cyber-physical system, eye–hand coordination, vision system, displacement sensors, pick/place

In this paper, we present an eye–hand coordination simulator for robot arms as a compact cyber-physical science, technology, engineering, and mathematics (STEM) learning unit that links visual perception to robot motion in pick/place interactions with a mobile robot as an automatic guided vehicle (AGV). The unit integrates four domains into one workflow: science (kinematics and motion), technology (sensors, motor controllers, vision), engineering (mechanisms and control states), and mathematics (geometric computation and frame transforms). The pick/place machine prototype includes linear X–Y–Z-axes with rotary and flip joints to realign an item box between a shelf and an AGV. A vision system detects a pair of fiducial circles to estimate the AGV centerline, yaw, and slot positions, while displacement sensors measure stand-off and assist parallel alignment. Performance was evaluated using a mock-up AGV positioned with varied offsets and yaw within a ±10 mm parking tolerance. Across 10 trials, the vision-based estimates of middle-slot X and stand-off S_x closely matched tape measurements, achieving 98–100% accuracy. The results show that the simulator is dependable in vision-guided coordination and usable as a simple, accessible platform for STEM education.

1. Introduction

Since the COVID-19 pandemic, online learning has become the best option to cope with the situation. However, online learning has a major weakness: the lack of in-person interaction with teachers and peers. This makes discussions and debates challenging. Certain lessons, such as laboratory work or hands-on practical skills, require face-to-face learning for a comprehensive understanding. To mitigate the shortcoming of the learning method, in this paper, we present the construction of lessons using a Science, Technology, Engineering, and Mathematics (STEM) education approach as cyber-physical lessons.

The STEM approach to education emphasizes the importance of enabling students to comprehend lessons and apply them in practice. In addition, cyber-physical systems are

*Corresponding author: e-mail: pitikhate.so@kmitl.ac.th
https://doi.org/10.18494/SAM5952

ISSN 0914-4935 © MYU K.K.
https://myukk.org/

increasingly becoming significant and popular worldwide. In this paper, we propose the creation of STEM lessons as a model for developing cyber-physical learning units by integrating scientific knowledge, technology, engineering design, and mathematics into this learning framework. In this study, we outline the design and control of robots using a vision system as a component to analyze the robot's movement and grasping positions. In these STEM lessons, it consists of Science (S) utilized to understand the robot movement, including the speed and traveling distance of the robot at each axis. Technology (T) involves learning how to use motor controllers for each axis, understanding and utilizing sensors, programming to control the robot, and operating the camera for the vision system. Engineering (E) focuses on designing robot structures based on their intended use and creating control states for robotic movement. Lastly, Mathematics (M) includes calculating aspect ratios to compare distances in millimeters and applying geometric theorems to determine the working distance for each robot axis.

In other words, in this research, we propose the development of a cyber-physical model for STEM education to facilitate learning about robots and vision systems through robot simulations. The content created is new and integrates knowledge of science, technology, engineering, and mathematics in the form of simulations. This approach enables learners or individuals interested in autonomous robots and vision systems to understand and visualize their practical applications. Furthermore, this knowledge can be utilized to design or control robots in various future applications. Unlike existing STEM learning kits that focus mainly on stationary pick/place tasks, our simulator integrates a mobile robot (AGV) docking process with a vision-guided robotic arm, thereby enabling learners to experience full cyber-physical coordination. This integration highlights the novelty of linking vision-based perception, AGV alignment, and real-time control in a unified STEM learning framework.

2. Related Work

In STEM education research, the use of robotics and vision systems as instructional media has attracted widespread attention because it enables hands-on learning, fosters analytical thinking, problem-solving, and teamwork skills, and helps students make the abstract concepts of science, technology, engineering, and mathematics more concrete.

2.1 STEM education

STEM education represents an interdisciplinary approach to learning that integrates knowledge and skills from these four subjects. STEM education encourages students to see the connections between them. By integrating theory with practical application, this approach helps learners build a deeper understanding of concepts and how they relate to real-world situations. Ultimately, students are better equipped to apply what they have learned in meaningful hands-on ways.[1–18]

2.2 Research related to STEM education approaches

In this subsection, we briefly review the STEM education literature to shape the applied learning unit developed here. Prior work shows that 3D printing that can be considered as a used-case of a Cartesian robot bridges theory and classroom prototyping.(3) Other studies describe microcontroller-based educational robots with multiple sensors (e.g., ultrasonic for obstacle detection) and a camera module as the vision system; students program behaviors such as turning, obstacle avoidance, and line following, which boosts motivation and deepens the understanding of STEM principles.(2) These examples of the studies suggest that learners can plan, design, and test models in engineering, science, and mathematics directly, while strengthening analytical thinking, creative problem solving, interdisciplinary teamwork, and habits of systematic experimentation.

2.3 Vision system for pick/place machine

The pick/place machine is a classic entry point for integrating vision with industrial or educational robots. The workflow runs from object perception through image–robot calibration to manipulation and lays the groundwork for reliable automation. Typical architectures for such machines can be categorized as follows.

2.3.1 Eye–hand calibration

Eye-hand calibration is the linchpin that connects the robot's "eye" to its arm, establishing the transform from the vision system's image frame to the robot's kinematic frame. Recent work has turned to learning-based 3D vision to curb cumulative error and improve robustness in real settings, which in turn yields significant gains in pick accuracy.(6) On the perception side, AI is used to learn from diverse images, including classifying parts before grasping, effectively serving as the robot's "brain". For pick/place tasks that must be fast and low-cost, lightweight models, such as MobileNet, enable real-time object detection and classification on small edge hardware, easing the bottleneck between perception and robot control.(10)

2.3.2 Eye-in-hand and eye-to-hand

Eye-in-hand (camera on the wrist) offers a close, flexible view of the object: the camera moves with the end-effector, so the system can track the task continuously. It suits high-precision work or tight spaces. The trade-offs are tougher cable routing and the need for accurate camera–robot calibration to map image coordinates correctly to the robot frame.

Eye-to-hand (fixed/overhead camera) provides a wide, stable field of view that captures the whole scene, such as a conveyor, and the robot, making it suitable when many parts arrive at once or in sequence. This setup typically requires careful calibration between the camera and the floor or conveyor so the view remains consistent. Its limitation is lower detail near the grasp point, and the camera must be placed to fully cover the area where parts pass.(17,18)

Systems that use RGB-D sensing together with deep visual recognition to estimate object pose and choose grasp points frequently adopt the eye-in-hand layout as well.(7) In our case, the robot must observe an AGV that does not park in exactly the same spot and may arrive with some yaw. Mounting the camera on the wrist (eye-in-hand) is therefore preferable, because it can follow the arm right up to the point of action.

From surveying current vision-system technologies, we find a wide range of choices tailored to different tasks. For STEM education, however, we deliberately select a simple vision pipeline so learners can understand how to compute coordinates from images and use them to control the robot arm and then build on that foundation.

Overall, the literature underscores the benefits of "robots for learning", especially when delivered as integrated, hands-on projects with tangible demonstrations.(1,4,12,13,15) Technically, the vision system is central to pick/place: from object recognition (e.g., MobileNet/RGB-D) and hand–eye calibration to motion control and reliability assessment.(6-11) In this study, our framework emphasizes simple, readable hardware (e.g., linear and/or rotary axes), automatic calibration, and metrics for both technical and learning outcomes serving as a bridge from the classroom to semi-industrial/semi-logistics applications.

3. Methodology

In this section, we propose the methodology involved in STEM education. The main contents aim to describe the feature of pick/place machine (M/C) and the integration of a vision system into the machine to specify the coordinates of "Mobile robot: AGV".

3.1 Mathematics: Geometry and torque calculation for pick/place M/C

In designing a machine, we must consider the working purpose and working area for equipment selection and the sizing of actuators. In our case, we design a machine used for picking and placing the item box illustrated in Fig. 1. An item box is rectangle and can hold a total of eight items. The item box must be exchanged from the left and right shelves to the AGV

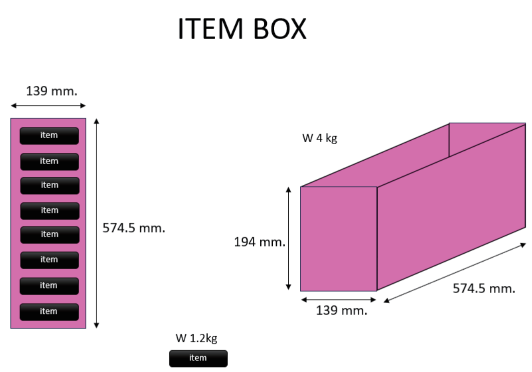

Fig. 1. (Color online) Item box sizing.

(a mobile robot) that runs to pick up the item box at the parking area in front of the machine as shown in Fig. 2.

The working space is 1.5 × 2 m^2. Figure 2 shows M/C working boxes with the need to exchange item boxes both from the left and right sides, including the front. Grippers must rotate around 180 degrees minimum to support the exchange position, shelf, and AGV.

From Fig. 3, the item box is placed horizontally, whereas the AGV receives the item box in a vertical position. Therefore, the M/C gripper must be able to flip the item box vertically and horizontally.

When analyzing the working characteristics and working area of the machine, we found that the M/C needs to move in the *X*- and *Y*-axes to receive and send workpieces to the shelf and

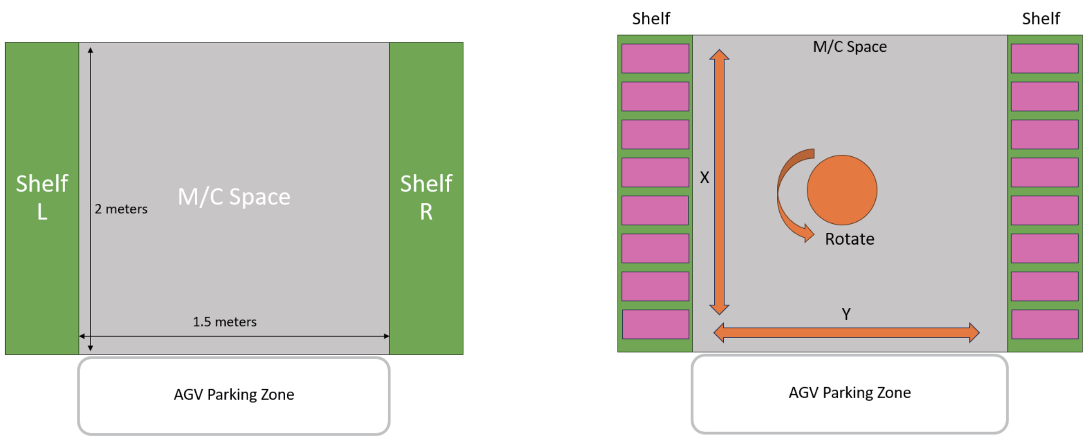

Fig. 2. (Color online) M/C spaces and working area for pick/place at shelf and AGV.

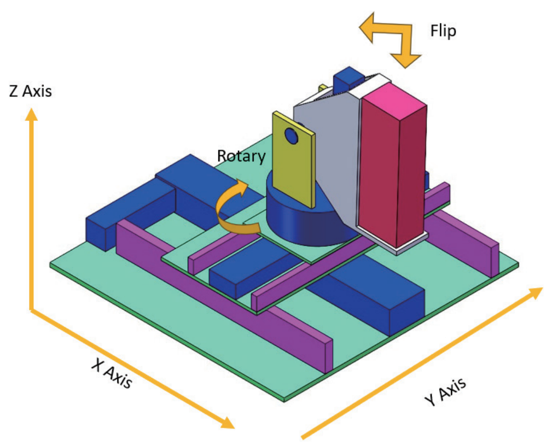

Fig. 3. (Color online) Pick/place machine (M/C).

AGV. Another necessary axis is the *Z*-axis to help adjust the height of placing equipment on the AGV's shelf and there is a rotary axis to allow the workpiece gripper to rotate in the desired direction at an angle of 180°. The last important axis is the flip axis to adjust the direction of the workpiece gripper to be able to place the item box horizontally and vertically.

Figure 4 shows the M/C model, which is designed from the working requirement. The lengths of the *X*-axis and *Y*-axis actuators depend on the working area, where the *X*-axis has an actuator length of 2 m and the *Y*-axis has an actuator length of 1.5 m.

The flip axis uses a rotary motor to rotate the gripper to move in a direction of 0–90°. It must have enough torque to lift heavy objects. The weight of the item box is 3.8 kg without any item, while each item weighs 1.2 kg. The item box can hold up to eight items, so the maximum and minimum weights of the load are 13.4 and 3.8 kg, respectively.

After identifying the maximum weight of the load, the suitable motor model can be selected. In doing so, the torque required for operation under the maximum load of 13.4 kg must be determined. For example, given the load shown in Fig. 4, where the weight (F) is 134 N and the distance from the pivot point (D) is 0.6 m, the required torque (τ) can be calculated as

$$\tau = FD, \tag{1}$$

$$\tau = 134x0.6, \tag{2}$$

$$\tau = 80.4\,Nm. \tag{3}$$

Therefore, the selection of the motor for the flip axis shaft requires a torque greater than 80.4 Nm.

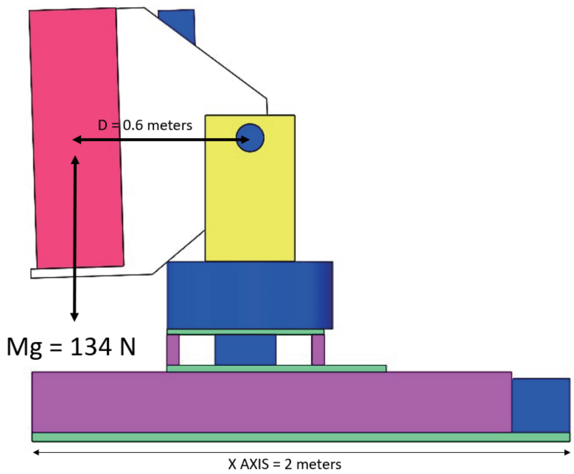

Fig. 4. (Color online) Setup for torque calculation and the flip axis (M/C).

3.2 Technology: AGV

The technology involved in this STEM context is a mobile robot or an AGV that was employed to exchange items according to the user's request. The AGV directly interacts with the M/C, as shown in Fig. 5. One AGV can send three item boxes, divided into Slots L, M, and R. Therefore, the capacity to exchange items at a time is 24 pieces per round. The AGV creates a map and determines the route to exchange the items from the users and pick/place machine, and each parking of the AGV has an uncertain position with a tolerance of ±10 mm.

Before exchanging items with the M/C, the AGV must send a signal, including AGV ID and Order Number, to request access and prevent exchange to the wrong AGV. If it is a different AGV ID, the M/C would reject the order and not allow the AGV to park, and if it is correct, the M/C sends a signal to allow the AGV to park in the parking zone.

When the AGV arrives at the parking spot, the AGV door automatically opens to allow the M/C to exchange item boxes. Each slot of the AGV consists of L, M, and R labels so that a camera installed in front of the M/C can detect the position of each slot via image processing.

3.3 Engineering: Operation state of M/C

The M/C operation was designed on the basis of the working requirement, which includes exchanging item boxes with the AGV. The overall operation of the M/C is in the form of automated storage, waiting to receive signal acquisition from users who request via the AGV. As shown in Fig. 6, when the AGV receives an order, it sends the order to the M/C to request withdraw items. When the M/C receives a request item list with an assigned AGV number that comes to pick up the workpieces, the M/C checks the number of workpieces in the warehouse to ensure correct quantity and then allow the AGV to park and dock to obtain the workpieces. However, if there are no items as requested, the M/C rejects the order and the AGV will leave the parking area.

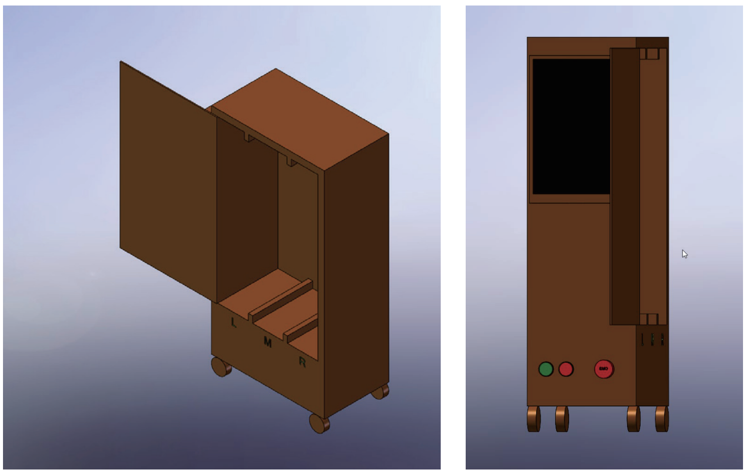

Fig. 5. (Color online) Mobile robot (AGV)

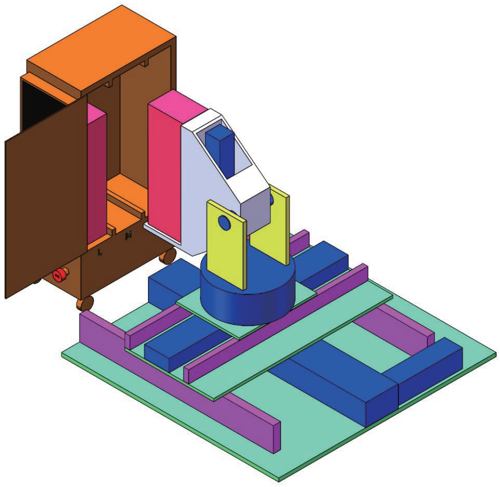

Fig. 6. (Color online) M/C and AGV interacting positioning.

In the exchange of items with the AGV, because the parking tolerance of the AGV is ±10 mm, there is a possibility that the AGV may park at an angle not perfectly parallel to the M/C, as shown in Fig. 7. These changes in parking position and orientation directly affect the handling of the items. Therefore, it is necessary to use a vision system to calculate the actual position of the AGV at that moment.

Figure 7 shows the possible parking positions of the AGV, with a defined tolerance zone for the parking area. If the AGV parks within the defined zone, and once the AGV is parked in the Parking Zone, the M/C will perform a self-alignment to orient the gripper head parallel to the plane of the AGV to pick up the item box.

3.4 Science: The experimental setup

To evaluate the effectiveness of the designed system, we set up an experiment to test the self-alignment in the situation that the misalignment occurred. To correct the misorientation after the AGV finished parking, the M/C needs to move itself to be parallel with the AGV. For this process, displacement sensors in Fig. 8 are used to measure the tilt of the AGV. The M/C is equipped with displacement sensors located at the far left and right ends of the gripper's range. These displacement sensors emit laser beams to measure the distance between the left and right positions, which are then used to calculate the tilt angle, as shown in Fig. 8. According to Fig. 8, the given $D1$ and $D2$ are the distances measured by the two displacement sensors, and the width is the distance between the two displacement sensors. When these values are calculated using the formula, the angle of the AGV can be determined. This angle is then used to adjust the rotary movement in order to align the gripper's position with the AGV as described by the equation

$$AGVRotation = \tan^{-1}\left(\frac{D1 - D2}{Width}\right). \tag{4}$$

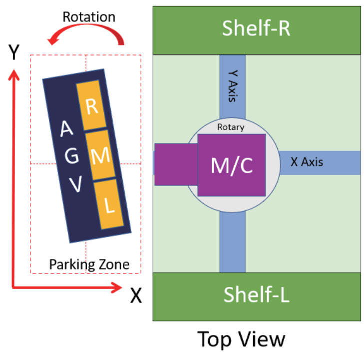

Fig. 7. (Color online) AGV parking position.

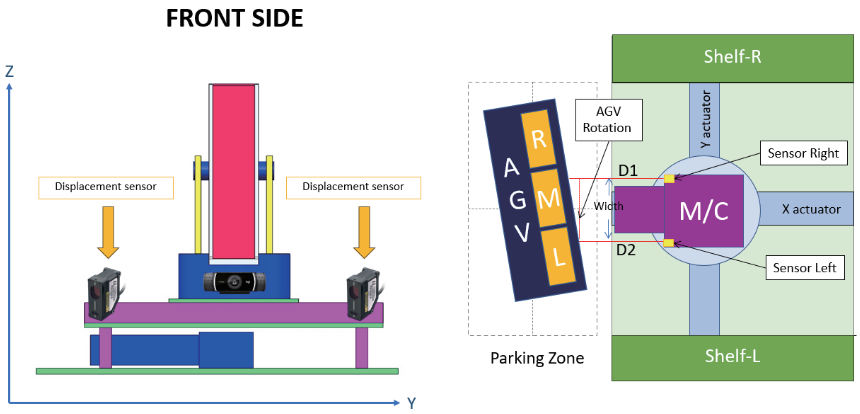

Fig. 8. (Color online) Experimental setup for self-alignment processes.

Prior to conducting the experiment, a camera calibration procedure was performed to ensure that the pixel coordinates in the captured images accurately corresponded to the real-world coordinates of the AGV and work area. A checkerboard pattern was created and placed on an AGV slot mock-up, replicating the geometry and dimensions of the actual docking slots. This mock-up served as a calibration reference for determining the camera's intrinsic parameters, including focal length, optical center, and lens distortion coefficients. Using the calibration results, the vision system could convert image-plane measurements into physical distances and angles with high accuracy. Consequently, the system was able to determine the AGV's centerline and tilt angle in real time, enabling precise alignment between the M/C gripper and the AGV slots.

In the next process, the center position of the AGV will be determined to calculate the position of each slot. This is because the AGV can place the item box in three positions: L (left), M (medium), and R (right).

If the AGV tilt exceeds a certain limit, the M/C will immediately reject the operation to prevent damage to the machine, as the M/C cannot adjust the tilt of the gripper. However, if the tilt is within the tolerance range, the system calculates the center position of the virtual line, which will then be used as the reference position for Slot M and serve as the reference point for positions R and L.

Once the center point of the virtual line is obtained, a perpendicular line will be drawn, and it will be compared with the camera's horizontal plane, which represents the image center line. If the virtual line and the image center line are offset, the M/C will adjust the Y-axis to move by the difference (Diff) to align with the center. In this context, the virtual line represents the AGV center, while the image center line represents the M/C pick/place center as shown in Fig. 9.

Once the M/C pick/place is in the center position of the AGV, the displacement sensor will be used to measure the distance between the M/C and the AGV. This distance is employed to adjust the *Y*- and *X*-axes for picking and placing the item box, and the length from the L and R offsets of the AGV orientation shown in Fig. 10 is used for calculation.

4. Results and Discussion

The results of the experiment using the vision system to determine the position of the AGV shown in Tables 1–3 were as expected. A mock-up AGV was created for testing purposes, and the mock-up was placed in different positions in front of the camera. The vision system captured the images and calculated the position, which was then compared with the actual value measured using a tape measure.

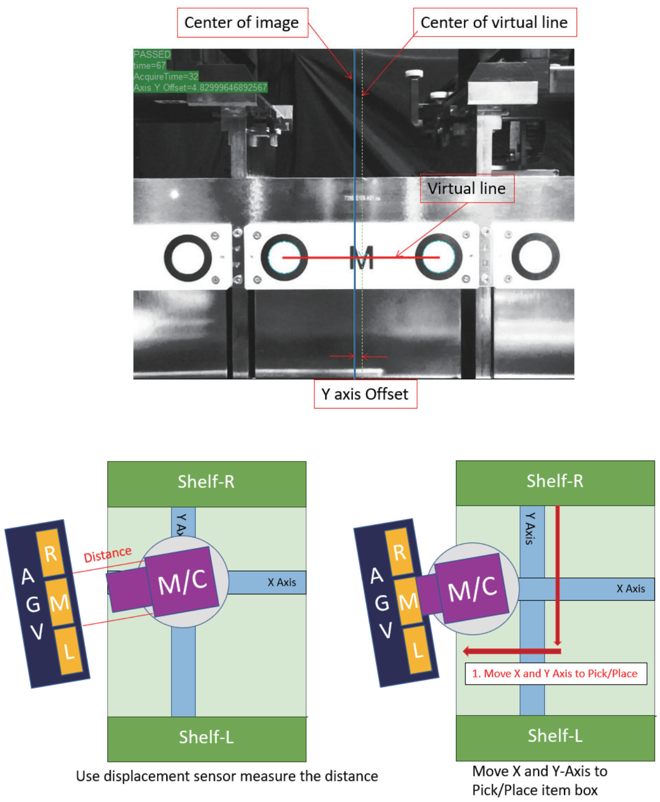

Fig. 9. (Color online) Pick/place calibration.

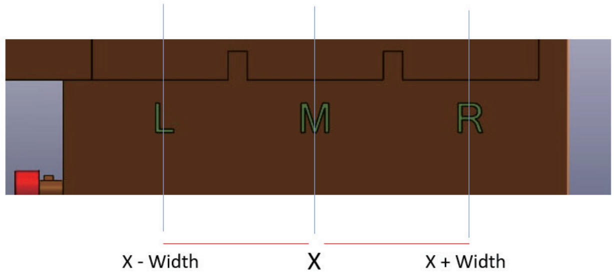

Fig. 10. (Color online) Width of the AGV slots.

Table 1
AGV coordinates (mm) obtained by calculating from the vision system. X: middle slot point; θ: AGV rotation; Sx: distance between AGV and M/C.

Round	X	θ	Sx
1	375.14	96.174	295.338587889
2	370.201	87.38	282.364531788
3	372.335	40.67	287.521318199
4	367.1749	65.452	297.191359523
5	373.2467	74.123	295.533587859
6	364.57	37.184	289.312897319
7	379.48	20.782	290.413179869
8	381.01	10.86	289.354331724
9	377.58	80.13	294.423881471
10	363.821	70.4854	296.723183839

Table 2
AGV coordinates obtained by measurement (real value) in experiment. X: middle slot point; Sx: distance between AGV and M/C.

Round	$X_{measure}$	$Sx_{measure}$
1	375	296
2	370	282
3	372	290
4	368	292
5	370	295
6	359	291
7	385	290
8	382	290
9	378	292
10	363	296

Table 3
Accuracy percentage (%) between Tables 1 and 2.

Round	$\%Accuracy$ of X	$\%Accuracy$ of Sx
1	99.96	99.78
2	99.95	99.87
3	99.91	99.14
4	99.78	98.22
5	99.12	99.82
6	98.45	99.42
7	99.57	99.86
8	99.74	99.78
9	99.89	99.17
10	98.77	99.76

In each round of measurement, the position of the AGV mock-up was adjusted to test the accuracy. It was observed that the actual measured distance and the distance calculated by the vision system closely matched, with a tolerance range of ±10 mm.

$$\textit{Accuracy Percentage}\ (\%) = [(\textit{Real Value} - \textit{Absolute Error}) / \textit{Real Value}] \times 100,$$

where $\textit{Absolute Error} = |\textit{Real Value} - \textit{Calculated Value}|$. The results are satisfactory.

Although the measured and calculated values showed high agreement, minor discrepancies between the two datasets can be attributed to the manual measurement process used for validation. The real values were obtained using a tape measure and visually read by human operators, which may introduce small reading errors due to parallax or alignment inaccuracy. In contrast, the vision system computes distances on the basis of calibrated image coordinates, which are inherently more repeatable and less subjective. Therefore, the slight deviations observed in some trials likely stem from human reading errors rather than system instability. Nevertheless, these deviations remain within the ±10 mm tolerance defined for AGV parking, confirming that the proposed system provides sufficient precision for STEM educational applications.

5. Conclusions

This STEM education in this study aims to demonstrate the use of a vision system in conjunction with a robotic arm, allowing the robotic arm to detect the position of objects for pick/place tasks. This is referred to as eye–hand coordination simulation, which serves as a prototype that can be used to create other robots utilizing vision systems as their "eyes".

The purpose of this STEM lesson is to showcase how to determine the position of objects. In this case, a model of a M/C is created to simulate a robotic arm. From the experiment, it was found that the vision system, combined with displacement sensors, can be used to determine the position of the AGV. The accuracy test, conducted over 10 rounds, showed that only one round had a slight deviation beyond the acceptable tolerance when comparing the measured distance to the actual distance.

Therefore, it can be concluded that this eye–hand coordination simulation can serve as a prototype for further development. To continue advancing this STEM education, a mock-up robot can be created to test actual pick/place operations using the real distances from the vision system to verify its functionality. Additionally, the installation distance of the displacement sensors and the positioning of the camera should be calculated carefully to ensure more accurate position measurements. Future work will integrate full robotic pick/place and optimize sensor placement to raise accuracy toward the implementation of a digital twin system. From an educational perspective, this simulator allows learners to visualize real-time coordination between sensors, actuators, and vision data, as well as interaction with other robots such as AGVs. Through hands-on practice, students gain practical insight into cyber–physical system concepts, enhancing their problem-solving and interdisciplinary thinking skills—key competencies in STEM education.

Acknowledgments

This research work's funding and access to facilities were supported by King Mongkut's Institute of Technology Ladkrabang (KMITL) [Grant number KREF016327]. We also thank the senior engineers at the first author's department and the workshop team at Seagate Technology Thailand for providing experimental space and lending equipment, including a mobile robot, cameras, and a robotic arm for testing.

References

1 Live Science: What is STEM Education? (2014). https://www.livescience.com/43296-what-is-stem-education.html (accessed Dec. 24, 2024).
2 Y. Sun and Q. Li: Proc. 2018 IEEE Int. Conf. Applied System Invention (ICASI), Chiba, Japan (2018) 1115–1118. https://doi.org/10.1109/ICASI.2018.8394476
3 Z. Mamatnabiyev: Int. J. Emerg. Technol. Adv. Eng. **14** (2024) 45. https://pdfs.semanticscholar.org/01db/6eee128c64b427757cac7636687000743cd5.pdf
4 H. Zhao and X. Lu: Open Educ. Res. (2016). https://en.cnki.com.cn/Article_en/CJFDTotal-KJYJ201606011.htm
5 A. K. Azad, A. Adhikari, P. Basnet, S. Timilsina, and S. Adhikari: Proc. 2023 IEEE Global Engineering Education Conf. (EDUCON), Kuwait City, Kuwait (2023) 1–6. https://doi.org/10.1109/EDUCON54358.2023.10112422
6 L. Li, X. Yang, R. Wang, and X. Zhang: J. Intell. Robot. Syst. **110** (2024) 130. https://doi.org/10.1007/s10846-024-02166-4
7 C.-S. Chen and N.-T. Hu: Sensors **23** (2023) 1076. https://doi.org/10.3390/s23031076
8 U. K. Sahu, M. K. S., A. K., M. Muzammil P, A. Jaiswal, U. K. Yadav, and S. K. Dash: Sci. Rep. **15** (2025) 13404. https://doi.org/10.1038/s41598-025-97930-3
9 H.-A. Phan, D. N. Bui, T. N. Dinh, B.-A. Hoang, A. N. Ngoc, D. T. H. Quoc, H. T. T. Ha, T. T. Bui, and V. N. T. Thanh: arXiv:2305.04605 (2023). https://arxiv.org/abs/2305.04605
10 F. Hong, D. W. L. Tay, and A. Ang: Electronics **12** (2023) 621. https://doi.org/10.3390/electronics12030621
11 J. B. Casella and M. Henderson: Robotic Arm Vision System with Pick/Place Operation, Penn State Behrend Senior Design Project (2021). https://sites.psu.edu/behrendseniordesign/2021/04/25/robotic-arm-vision-system-with-pick-place-operation-2/
12 I. Torres and E. Inga: Information **16** (2025) 96. https://doi.org/10.3390/info16020096
13 F. Ouyang and W. Xu: Int. J. STEM Educ. **11** (2024) 6. https://doi.org/10.1186/s40594-024-00469-4
14 A. Torres, A. Soliman, T. Isabell, J. Blackburn, L.-F. Wu, M. Sakamoto, A. Lilamwala, A. Neman, C. Bobadilla, M. Chen, A. Padmanabhuni, E. Stonestreet, J. Hazboun, X. Hai, R. Novitski, N. Mentzer, M. Rastgaar, and N. Mahmoudian: J. Form. Des. Learn. **9** (2025) 77. https://doi.org/10.1007/s41686-025-00102-9
15 P. Choudhary: IJA RSCT (2024). https://www.researchgate.net/publication/386539969_Robotics_in_STEM_Education_Enhancing_Engagement_Skills_and_Future_Readiness
16 E. J. Markvicka, J. D. Finnegan, K. Moomau, A. S. Sommers, M. S. Peteranetz, and T. A. Daher: ASEE Annu. Conf. & Expo (2023). https://smr.unl.edu/papers/Markvicka_et_al-2023-asee.pdf
17 S. Hutchinson, G. D. Hager, and P. I. Corke: IEEE Trans. Robot. Autom. **12** (1996) 651. https://doi.org/10.1109/70.538972
18 N. Lai, Y. Chen, J. Liang, B. He, H. Zhong, and Y. Wang: Mechatronics **82** (2022) 102724. https://doi.org/10.1016/j.mechatronics.2021.102724

About the Authors

Pimpran Preedanont received her B.S. degree in automation engineering from King Mongkut's Institute of Technology Ladkrabang, Thailand. Her research interests are in cyber-physical applications and STEM prototypes in robotics and AI. (63601044@kmitl.ac.th)

Pitikhate Sooraksa is a professor at the School of Engineering, King Mongkut's Institute of Technology Ladkrabang, Thailand. He received his B.Ed. (Hons) and M.Sc. degrees in physics from Srinakharinwirot University, Thailand, his M.S. degree from George Washington University, USA, in 1992, and his Ph.D. degree from the University of Houston, USA, in 1996, both in electrical engineering. His research interests include cyber-physical applications and rapid prototypes in robotics and AI.
(pitikhate.so@kmitl.ac.th)